Seasonal and spring interannual variations in satellite-observed chlorophyll-*a* in the Yellow and East China Seas:
new datasets with reduced interference from high concentration of resuspended sediment

Hisashi Yamaguchi[a], Joji Ishizaka[b], Eko Siswanto[c], Young Baek Son[d], Sinjae Yoo[e], Yoko Kiyomoto[f]

[a]Japan Aerospace Exploration Agency, Tsukuba Space Center, 2-1-1, Sengen, Tsukuba, Ibaraki, 305-8505, Japan
[b]Hydrospheric Atmospheric Research Center, Nagoya University, Furo-cho, Chikusa-ku, Nagoya, Aichi, 464-8601, Japan
[c]Japan Agency for Marine-Earth Science and Technology, 2-15, Natsushima-cho, Yokosuka, Kanagawa, 237-0061, Japan
[d] Korea Ocean Satellite Center, Korea Ocean Research & Development Institute, Ansan, P.O.Box 29, 425-600, Korea
[e]Korean Ocean Research and Development Institute, Korea
[f]Seikai National Fisheries Research Institute, 1551-8 Taira-machi, Nagasaki 851-2213, Japan

Corresponding author: Hisashi Yamaguchi (yamaguchi.hisashi@jaxa.jp)

Keywords: Yellow Sea; East China Sea; SeaWiFS; Chlorophyll-*a*; Total suspended matter; Local algorithm; Spring bloom

Abstract

Seasonal and spring interannual variations in chlorophyll-*a* (Chl) and total suspended matter (TSM) in the Yellow and East China Seas through a 10-year period were examined by using new datasets from Yellow Sea Large Marine Ecosystem Ocean Color Project (YOC) algorithms. YOC SCHL calculations are based on a combination of the SeaWiFS standard algorithm and a local empirical algorithm for areas of low and high normalized water-leaving radiance 555 nm, respectively. YOC SCHL was lower than the standard SCHL in areas with high concentrations of resuspended sediment, especially along the Chinese and Korean coasts and around the Changjiang Bank from fall to spring. YOC SCHL was high in areas of low TSM in the middle of the Yellow Sea, and offshore of the Changjiang Bank in April, indicating the occurrence of spring blooms. In these areas, TSM was dominated by phytoplankton cells and phytoplankton-related organic particles. Offshore from the Changjiang River mouth and around the Changjiang Bank, YOC SCHL and TSM in March were low and high, respectively, with maximum YOC SCHL values occurring around the Changjiang Bank in May. Spring bloom started with decreases in resuspended sediment concentrations in these areas. During summer, YOC SCHL values were high and TSM concentrations were low; TSM was dominated by organic particles related to phytoplankton activity when Changjiang River diluted water moved from the river mouth to east of the bank. YOC SCHL in spring offshore from the Changjiang River mouth increased significantly during the 10 years, and correspond to an increase in red tide events. In the middle of the Yellow Sea, maximum YOC SCHL in spring increased gradually and significantly during the 10 years. Many of the spatial and temporal variations in YOC SCHL were consistent with a range of earlier *in situ* descriptions. Our results indicate that the satellite ocean data with proper algorithms is a powerful tool to analyze phytoplankton dynamics in moderate-high suspended sediment area.

1. Introduction

The Yellow and East China Seas (hereafter, YECS) are marginal seas surrounded by Japan, China, and Korea. The YECS is connected to the South China Sea, Pacific Ocean, and Sea of Japan by the Taiwan Strait, the strait between Taiwan and the Ryukyu Islands, and the Tsushima Strait, respectively. Most of the YECS consists of shallow continental shelf (< 200 m) (Fig. 1). The Changjiang River, one of the world's largest rivers, supplies large amounts of fresh water and sediment to the YECS, especially during summer.

From fall to early spring, turbidity is high in shallow areas of the YECS (< 50 m), resulting from strong northeast monsoon activity that causes vertical mixing of the water column and sediment resuspension from the bottom (Xie et al., 2002). The resuspended sediment may dominate total suspended matter (TSM) in this area, although organic particulate matter related to biological activity, such as phytoplankton production, is likely not negligible in some cases.

Phytoplankton is the base of the marine food chain, and chlorophyll-*a* (Chl) is an index of the amount of phytoplankton. Growth of phytoplankton requires nutrients and a favorable light environment for photosynthesis. In coastal area, suspended sediment is often one of the major factors for controlling phytoplankton, and it is important to understand the relationship to phytoplankton dynamics (Cloern, 1996).

Ocean color satellite imagery is useful for understanding spatial and temporal variations in Chl. Kim et al. (2009) examined the standard ocean-color product of the

Sea-viewing Wide Field-of-view Sensor (SeaWiFS) and found that the distribution of standard satellite Chl (SCHL) in summer corresponded to Changjiang River Diluted Water (CDW) in the East China Sea. Yamaguchi et al. (2012) also demonstrated that the movement of the summer maximum of standard SeaWiFS SCHL from the Changjiang River mouth to farther offshore corresponded with the extent of CDW.

Spring blooms are important events in the seasonal variation of Chl in temperate coastal ecosystems and are likely also important in the YECS. It has long been hypothesized that initiation of phytoplankton blooms is related to the relationship between the critical depth and the mixed layer depth (Sverdrup, 1953), and it is suggested that it is also important in turbid coastal water (Fichez et al., 1992). Yamaguchi et al. (2012) detected the presence of a spring bloom by using maximum values of standard SCHL and low values of normalized water-leaving radiance (nLw) at 555 nm (nLw555) as an index of suspended sediment. However, variation in the spring bloom throughout the whole YECS was difficult to determine by standard SCHL, which is likely distorted by high concentrations of resuspended sediment in Chinese and Korean coastal areas and around the Changjiang Bank from late fall to early spring.

On longer time scales, Chl may change interannually owing to climate oscillation, climate change, and anthropogenic environmental changes. Increases in red tide events and massive outbreaks of giant jellyfish have recently occurred in the YECS, and eutrophicasion is suspected as a possible cause (e.g., Kawahara et al., 2006; Siswanto et al., 2008; Zhou et al., 2008). These events suggest that the environment in the YECS may

be changing. Yamaguchi et al. (2012) demonstrated that interannual variation in summer standard SCHL is controlled by interannual variation in the Changjiang River discharge into the East China Sea. They also showed that summer standard SCHL has been gradually increasing in the Yellow Sea, where the influence of the variation of discharge was not high. However, both the seasonal SCHL variation and the interannual variation in spring standard SCHL over the whole YECS area are difficult to determine because of interference caused by resuspended sediments.

It is difficult to use ocean color remote sensing for observing Chl in high suspended sediment area because there is no good atmospheric correction algorithm due to accuracy of the aerosol and bio-optical models (Jamet et al., 2011). Siswanto et al. (2011) recently developed new empirical local algorithms for the YECS by using YOC *in situ* Chl and satellite optical data. They optimized the Tassan Chl algorithm for high nLw555 waters. The locally-tuned Tassan Chl algorithm is less influenced by high nLw due to suspended sediment than the standard SeaWiFS Chl algorithm (Siswanto et al., 2011). The locally-tuned Tassan Chl algorithm is applied to SeaWiFS nLw data processed using standard (Case 1) atmospheric correction. Siswanto et al. (2011) recommend combinations of the standard and YOC SCHL algorithms under low and high nLw555 conditions (2 mW cm^{-2} um^{-1} sr^{-1}), respectively. They also developed an empirical TSM algorithm for this region. However, they demonstrated performance only by fitting the output to *in situ* data and did not explore spatial and temporal variations in the calculated SCHL and TSM.

The objective of our study was to describe spatial and temporal variations in SeaWiFS-based YOC SCHL and TSM using a method that reduces overestimation of SCHL in waters with high resuspended sediment concentrations. In addition, we compared our results with previous field observations to demonstrate consistency. Here, we describe seasonal variations in YOC SCHL and TSM for comparison with standard SCHL estimates. We then describe interannual variations in springtime YOC SCHL and TSM, and the consistency between our estimates and field observations. The ratio of YOC SCHL to TSM was used to estimate the abundances in TSM of resuspended sediment and organic particles derived from phytoplankton.

2. Material and Methods

Daily nLw of 412, 443, 490, 555, and 670 nm data from NASA SeaWiFS (Reprocessing 5.1 version) Level 2 Global Area Coverage (GAC) during January 1998 and December 2007 were used to calculate remote-sensing reflectance (R_{rs}). The data had a spatial resolution of 4 km. The OC4v4 algorithm was used to calculate standard SCHL (O'Reilly et al., 2000). For the new local algorithm (YOC SCHL; Siswanoto et al., 2011), we used a Tassan-like algorithm and an OC4v4 algorithm for high (>2.5 mW cm^{-2} um^{-1} sr^{-1}) and low (<1.5 mW cm^{-2} um^{-1} sr^{-1}) ranges of nLw555, respectively. The Tassan (1994)-like SCHL algorithm is based on computation of three component optical models, which are absorption and backscatter of Chl, TSM and colored dissolved organic matter, referring to Prieur and Sathyendranath (1981).

The algorithm is as follows:

$$\mathrm{SCHL} = 10^{\left(-0.166-2.158Log_{10}(R)+9.345Log_{10}^{2}(R)\right)},$$

where

$$\mathrm{R} = \left(\frac{\mathrm{Rrs}_{443}}{\mathrm{Rrs}_{555}}\right)\left(\frac{\mathrm{Rrs}_{412}}{\mathrm{Rrs}_{490}}\right)^{-0.463}$$

.

The first term is sensitive to Chl because Rrs_{443} and Rrs_{555} are close to the Chl absorption maximum and minimum, respectively. The second term consists of Rrs_{412} and Rrs_{490}, shorter and longer wavelength of the Chl absorption maximum, respectively. This is the compensating term, which is the low dependence on Chl and high dependence on absorption of suspended sediments and colored dissolved organic matter (Fig. 1 of Tassan, 1994). Siswanto et al. (2011) suggested that, because atmospheric correction for high nLw water is a serious source of error, adjustment to satellite Rrs is necessary for better SCHL estimation. Thus, they optimized the algorithm by using *in situ* Chl and satellite Rrs in high nLw555 (>2.0 mW cm^{-2} um^{-1} sr^{-1}) ocean areas. They demonstrated that overestimation of Chl in high nLw water is significantly reduced, and showed that the error caused by the standard atmospheric correction in high nLw water can also be reduced by tuning. A linear combination of the two algorithms was used for mid-range nLw555 (2.5 mW cm^{-2} um^{-1} sr^{-1} > nLw555 > 1.5 mW cm^{-2} um^{-1} sr^{-1}) to ensure a smooth data transition.

TSM was also calculated using another Tassan-like algorithm:

$$TSM = 10^{\left(0.649+25.623(Rrs_{555}+Rrs_{670})-0.646\left(\frac{Rrs_{490}}{Rrs_{555}}\right)\right)}.$$

The SeaWiFS Data Analysis System (SeaDAS version 5.4) was used to calculate R_{rs}, Chl, and TSM from nLw. Monthly composites for each year and the 10-year averages were calculated using Windows Image Manager (WIM) software (http://www.wimsoft.com/). Statistical analysis by Spearman's rank correlation was used to detect the springtime interannual trends of SCHL and TSM.

3. Results

3.1. Spatial Distributions of Standard and YOC SCHL and TSM

The 10-year averages of monthly standard SCHL were high in the Bohai Sea along the Chinese and Korean coasts. In January, a tongue-shaped high SCHL structure extended southeastward along the 50-m isobath around the Changjiang Bank (Fig. 2A). However, YOC SCHL was lower (1.0–5.0 mg m^{-3}) than standard SCHL (2.0–10.0 mg m^{-3}) in areas of high TSM (2–19 g m^{-3}). The tongue-shaped water mass had high TSM and low Chl by YOC SCHL calculations. In April, standard SCHL was high (1.3–10 mg m^{-3}) throughout the Bohai Sea and YECS (Fig. 2B). YOC SCHL was high (0.8–10 mg m^{-3}) only in the middle of the Yellow Sea and east and south of the Changjiang Bank, where TSM was low. The high YOC SCHL and low TSM area probably corresponded to the area of the spring bloom. YOC SCHL was lower than standard SCHL around the Changjiang Bank, where TSM was high (2–6 g m^{-3}).

In July, the tongue-shaped high SCHL structure extending northeastward from offshore of the Changjiang River mouth to around the Changjiang Bank was observed by both the standard and YOC SCHL (Fig. 2C). TSM was higher in this area than in the surrounding areas (1–4 g m^{-3}) but not as high as in the coastal area. Differences between standard SCHL and YOC SCHL were obvious only in coastal areas of Jiangsu Province and near the mouth of the Changjiang River, where TSM was high (>15 g m^{-3}).

The tongue-shaped high standard SCHL structure, which had extended northeastward in July, shifted to extend southeastward in October (Fig. 2D). However, the structure was not observed by YOC SCHL. Areas with large differences between standard and YOC SCHL and areas of high TSM were similar to those in January.

The distribution of the ratio YOC SCHL/TSM was very similar to the distributions of TSM and the difference between standard and YOC SCHL. The SCHL/TSM ratio was low (<1/1000) along the Bohai Sea coast off China and Korea and offshore of the Changjiang River mouth in January, April, and October. In July, the SCHL/TSM ratio was low only along the Chinese coast. In these low SCHL/TSM regions, TSM may be mostly composed of resuspended sediments; in other regions with similar ratios, TSM may be mostly derived from phytoplankton, as discussed below.

3.2. Seasonal Variation in Monthly YOC SCHL and TSM

Along the 124.5°E longitude line (27.5–37.5°N), the 10-year average of monthly YOC SCHL was high (>1 mg m^{-3}) from March to May, and TSM was low (<2 g m^{-3})

from June to August over the YECS (Fig. 3A). Maximum YOC SCHL (>2 mg m^{-3}) was observed in the middle of the Yellow Sea from 34.7 to 36°N latitude in April. Maximum YOC SCHL (>1 mg m^{-3}) was also observed south of the Changjiang Bank around 29.5°N from March to May. These maxima indicate the occurrence of a spring bloom. Around the Changjiang Bank from 31.5 to 33.0°N, TSM was high (>2 g m^{-3}) in winter, rapidly decreased from April, and then increased from September. On the other hand, high YOC SCHL (>2 mg m^{-3}) was observed from May in this area, decreased from September, and then remained constantly low during winter. This indicates that resuspension of sediment was high and phytoplankton was not abundant in the area during winter. Starting in May, phytoplankton became abundant after settlement of the sediment.

Along the 31.75°N line from near the Changjiang River mouth to east of the Changjiang Bank (122–128°E), both YOC SCHL and TSM were generally high to the west, decreasing gradually to the east. However, both had distinct seasonal variations. TSM was very high (>10 g m^{-3}) near the river mouth to the west of 122.2–122.6°E. High concentrations of TSM (> 2 g m^{-3}) extended to the east of the Changjiang Bank at 126.5°E from winter to early spring (Fig. 3B); high concentrations were limited to 123.5°E during summer. High YOC SCHL concentrations (>3 mg m^{-3}) extended to 124.0°E during summer. The YOC SCHL concentration near the river mouth (5 mg m^{-3}) (122–122.5ºE) was lower than the concentration offshore from the mouth (11 mg m^{-3}) (122.8°E) in July. Two seasonal maxima occurred around the Changjiang Bank at 124.5°E and to the east of the Changjiang Bank between 125° and 126.5°E in spring and summer, and in spring

and fall, respectively.

The 1° × 1° area-averaged 10-year average of monthly YOC SCHL and TSM in the middle of the Yellow Sea showed maximum values in April (SCHL: 1.9 mg m^{-3} and TSM: 1.2 g m^{-3}) (Fig. 4A). A similar spring maximum was observed south of the Changjiang Bank (SCHL: 1.6 mg m^{-3} and TSM: 1.0 g m^{-3}) (Fig. 4B). Correlations between YOC SCHL and TSM were positive in the middle of the Yellow Sea and south of the Changjiang Bank (SCHL/TSM = 1/758; r = 0.93, $p < 0.01$; and SCHL/TSM = 1/780; r = 0.89, $p < 0.01$; Fig. 5A and B, respectively). These values for the SCHL/TSM ratio were close to those of the phytoplankton-dominated TSM (1/275~1/600) reported by Kishino et al. (2005). In these two areas, the seasonal variation in TSM was low (<2 g m^{-3}) throughout the year, and the variation was likely caused by particles related to phytoplankton.

From offshore of the Changjiang River mouth to east of the Changjiang Bank, monthly YOC SCHL and TSM decreased with distance from shore (Fig. 4C, D, and E). Seasonal maximums of YOC SCHL in areas offshore of the river mouth (Fig. 4C), around the bank (Fig. 4D), and east of the bank (Fig. 4E) were observed in July (7.7 mg m^{-3}), May and August (2.0 and 2.3 mg m^{-3}), and April and August (1.0 and 0.8 mg m^{-3}), respectively. In the same areas, seasonal maximums of TSM were observed in January (8.7 g m^{-3}), February (7.1 g m^{-3}), and January (1.7 g m^{-3}), respectively.

Offshore from the Changjiang River mouth, YOC SCHL was constantly low (~1.5 mg m^{-3}) from January to March when TSM was high, and YOC SCHL increased with

decreasing TSM from April to June (2.3–4.8 mg m^{-3}) (Fig. 5C). The winter SCHL/TSM ratio was low (<1/1000) when resuspension of sediment was high. The increase in YOC SCHL started when TSM fell to less than 5 g m^{-3} in April. Maximum YOC SCHL and summer maximum TSM values occurred in July, and the YOC SCHL/TSM ratio (1/454) in July was closely similar to that in the middle of the Yellow Sea and south of the Changjiang Bank. YOC SCHL decreased after the July maximum with less change in TSM. From October, YOC SCHL decreased with an increase in TSM.

YOC SCHL also increased with the decrease in TSM from April to May (1.38–1.97 mg m^{-3}) around the bank (Fig. 5D). In this area, YOC SCHL also started to increase when TSM became less than 5 g m^{-3} in April; maximum YOC SCHL occurred in May, but the increase was relatively small. Winter SCHL/TSM was low (<1/1000), indicating the presence of high concentrations of resuspended matter on this shallow offshore bank. From June to August, SCHL/TSM reached levels (1/582) close to those for the middle Yellow Sea and south of the Changjiang Bank. The increase in YOC SCHL around the bank was lower than that found offshore of the Changjiang River mouth. The YOC SCHL decreased with an increase in TSM from October.

East of the bank, YOC SCHL slightly increased with the decrease in TSM from winter to spring and then decreased with decreasing TSM from June to August (SCHL/TSM = 1/699) (Fig. 5E).

3.3 Interannual Variation in YOC SCHL and TSM in Spring

Maximum values of monthly YOC SCHL in the middle of the Yellow Sea (1.5–3.0 mg m^{-3}) and south of the Changjiang Bank (1.2–3.5 mg m^{-3}) from February to June in 1998 to 2007 were observed in March and April (Fig. 6A and B). Monthly TSM was low (0.2–1.7 g m^{-3}) in those areas from February to June, and TSM did not appear to control the spring bloom. The spring maximum of YOC SCHL significantly increased over the 10 years in the middle of the Yellow Sea (ρ= 0.62, p = 0.05). However, south of the Changjiang Bank, the maximum of spring YOC SCHL did not show an increasing trend.

On the other hand, the monthly YOC SCHL from February to June reached maximum values offshore of the Changjiang River mouth (2.9–12.2 mg m^{-3}) and around the bank (1.9–3.3 mg m^{-3}) in April, May, and June (Fig. 6C and D). Monthly TSM in those areas had maximum values (3.8–12.9 g m^{-3}) in February or March, and YOC SCHL increased after the decrease in TSM in spring. The monthly YOC SCHL from April to June in 2000–2007 was higher than that in the period 1998–1999 offshore of the Changjiang River mouth. The average YOC SCHL tracked a significantly increasing trend (ρ=0.70, p = 0.03) from April to June. Around the bank, YOC SCHL did not show a significant trend in spring.

East of the bank, YOC SCHL from February to June showed maximum values (0.7–1.3 mg m^{-3}) in March, April, and May throughout the 10 years (Fig. 6E). The average YOC SCHL from March to May increased significantly (ρ= 0.62, p = 0.05). Maximum monthly TSM in this area (0.7–2.4 g m^{-3}) occurred in February or March, and average

TSM from February to March decreased significantly during the 10 years (ρ= - 0.92, p < 0.001).

4. Discussion

4.1. Differences between Standard and YOC SCHL

YOC SCHL was lower than standard SCHL across large areas of Chinese and Korean coastal waters and around the Changjiang Bank (Fig. 2). Those areas corresponded to high TSM areas, and standard SCHL was expected to overestimate actual Chl concentrations because of the high resuspended sediment concentrations. Kiyomoto et al. (2001) used Coastal Zone Color Scanner and Ocean Color and Temperature Scanner data to compare *in situ* Chl and SCHL around the Changjiang Bank in winter and suggested that SCHL was overestimated due to resuspension of sediment.

Several atmospheric correction algorithms for turbid water are proposed. Jamet et al. (2011) compared three different SeaWiFS atmospheric correction algorithms for turbid water. One is SeaWiFS standard algorithm since 2009 based on a bio-optical model and an iterative process, another is based on the spatial homogeneity of near- infrared rations of the aerosol and water leaving radiance and the other is based on a fully coupled atmosphere and ocean spectral optimization inversion. They reported that SeaWiFS standard atmospheric correction algorithm was more accurate than other algorithms. However that algorithm was not sufficient the requirement level of accuracy. Hu et al. (2000) proposed the “nearest neighbor” atmospheric correction method in high TSM area,

which algorithm is assumed that aerosol condition of turbid water and the near clear water are uniform; however, that method requires the some pixel of case 1 water nearby.

Our analysis of SeaWiFS data demonstrated that YOC SCHL was lower in all seasons than standard estimates for large areas of high TSM water. Therefore, YOC SCHL reduces the overestimation effect of high TSM. The approach of Siswanto et al. (2011) reduces error by application of a simple empirical algorithm with SeaWifS standard nLw. Although the algorithm is certainly not the perfect solution, at present, it may be one of the best approaches because there is no good atmospheric correction algorithm currently available. Indeed, as we discuss below, the behaviors of Chl and TSM using this approach are reasonably consistent with previous descriptions for the study area. Verification of the procedure with a larger *in situ* data set is certainly required.

4.2. Seasonal Variations in YOC SCHL and TSM

The 10-year-averaged monthly YOC SCHL was high in the middle of the Yellow Sea and south of the Changjiang Bank, with low TSM in April (Fig. 4A, and B, respectively). Typical spring blooms occurred in these two areas. There was a positive correlation between TSM and YOC SCHL in the middle of the Yellow Sea and south of the Changjiang Bank (Fig. 5A and B, respectively). Kishino et al. (2005) reported a relationship between Chl and minimum TSM in Tokyo Bay, which may indicate the relationship between Chl and weight of phytoplankton and other organic particles related to phytoplankton (Chl/TSM = 1/275~1/600). The slopes of regression lines between TSM

and YOC SCHL in the middle of the Yellow Sea and south of the bank (SCHL/TSM = 1/758 and 1/780) were similar to that relationship. Thus, resuspended sediment concentrations were minimal in these areas, and organic particles produced by biological activity were dominant.

In contrast to the middle of the Yellow Sea and south of the Changjiang Bank, TSM was high offshore of the Changjiang River mouth and around the Changjiang Bank from fall to early spring (Fig. 5C and D). The bottom sediment in these low SCHL/TSM (<1/1000) areas was dominated by fine particles, and resuspension was caused by vertical water mixing resulting from strong winter monsoon activity (Zhu and Chang, 2000; Xie et al., 2002) (Fig. 2). Yang et al. (2007) also reported high surface TSM (>4 g m^{-3}) in the well-mixed water column around the Changjiang Bank after a storm. Our study demonstrates that high TSM and low SCHL/TSM areas correspond well with the area of sediment resuspension between fall and early spring. TSM decreased to less than 5 g m^{-3} and YOC SCHL subsequently increased from April onward. The increase in YOC SCHL and decrease in TSM continued until May in these areas. Zhu et al. (2009) detected light limitations for phytoplankton growth in spring seaward from close to the Changjiang River mouth (122°E–123.6°E) by analyzing correlations between *in situ* Chl and the ratio of euphotic depth to surface mixed layer depth. Our estimates for the areas offshore from the Changjiang River mouth and around the Changjiang Bank were consistent with calculations of Zhu et al. (2009), i.e., the increase in SCHL started after resuspended sediment concentration decreased in April. Phytoplankton growth may be controlled by

light availability until March when there are high resuspended sediment concentrations in the water;, the spring bloom may start in April when the critical depth becomes deeper than the mixed layer depth as suspended sediment concentrations decrease (cf. Zhu et al., 2009, Cloern, 1987). Spring YOC SCHL values offshore from the river mouth were higher than around the bank because surface nutrients at the river mouth are higher than around the bank in winter (Jiao et al., 2005). To the east of the bank, light control of the spring bloom by resuspended sediments may have been less effective because TSM was relatively low (<5 g m^{-3}) (Fig. 5E).

In summer, TSM was high near the mouth of the Changjiang River and rapidly decreased seawards. Maximum YOC SCHL (>11 mg m^{-3}) was observed offshore of the mouth (around 122.8°E, Fig. 3B). *In situ* surface Chl is higher offshore (> 10 mg m^{-3}) than near the mouth (> 1-4 mg m^{-3}) of the Changjiang River (Chen et al., 2003; Zhu et al., 2009). Zhu et al. (2009) reported that large amounts of fresh water from the Changjiang River supply abundant nutrients and sediments during summer. They observed diatom-dominated assemblages in high *in situ* Chl (> 10 mg m^{-3}) waters occurring in the high nutrient, low turbidity area beyond the Changjiang River front at 122.5°E and 123°E. Our results are consistent with those of Chen et al. (2003) and Zhu et al. (2009). We measured low Chl near the mouth, likely due to low light conditions caused by high resuspended sediment concentration; Chl increased farther offshore as light increased with declining resuspended sediment concentration.

YOC SCHL near the mouth of the Changjiang River was lower than offshore from

the mouth and was likely controlled by low light conditions. Nevertheless, values were still higher than 5 mg m^{-3} near the mouth, perhaps because of an abundance of dinoflagellates under reduced light conditions (Zhou et al., 2008). Dinoflagellates are able to photosynthesize and grow through their ability to swim into the shallow euphotic zone, where they can form red tides in these water masses. Maximum YOC SCHL in summer occurred offshore from the mouth, around the bank, and east of the bank in July, August, and August, respectively (Fig. 4C, D, and E). Kim et al. (2009) reported that high standard SCHL in summer corresponded with low salinity water, and Yamaguchi et al. (2012) also showed that over a roughly two-month period, CDW can be traced with the seasonal maximum of standard SCHL extending east of Jeju Island from offshore of the Changjiang River mouth. The maximum YOC SCHL we measured matched the maximum standard SCHL reported by Yamaguchi et al. (2012), indicating movement of the CDW. TSM and YOC SCHL had positive linear correlations in the track of CDW movements during summer (Fig. 5C, D, and E). The slope of the regression line of SCHL/TSM was similar to those for the middle of the Yellow Sea and south of the Changjiang Bank. We found reduced resuspended sediment concentrations in the CDW, where phytoplankton and related organic particles dominated the TSM.

YOC SCHL was higher offshore from the Changjiang River mouth than around and to the east of the Changjiang Bank. This result indicates that phytoplankton abundance was high in this area because of the large quantity of nutrients supplied by the Changjiang River and upwelling of bottom Taiwan warm current water (Chen et al., 2003;

Gong et al., 2003). From October, SCHL decreased with increasing TSM in areas offshore from the river mouth and around the bank. It is likely that the critical depth became shallower than the mixed layer depth as the mixed layer depth and resuspended sediment concentration increased in these areas.

4.3. Spring Interannual Variations in YOC SCHL and TSM

YOC SCHL increased offshore from the Changjiang River mouth from 2000, and especially high YOC SCHL (>14 mg m^{-3}) was observed in June 2003 (Fig. 6C). Nitrate input from the river has been increasing dramatically since the 1960s, and an increasing trend in phytoplankton standing stock occurred in these areas from 1984 to 2002, particularly in late spring (Zhou et al., 2008). Both in number and scale, harmful algal blooms (HABs) have also increased dramatically in these areas since 2000 (Wang, 2006). Furthermore, the timing of HAB occurrence shifted during the period from 1933 to 2004: HABs occurred from August to October before the 1980s, in July-August in the 1980s, during May-July in the 1990s, and in May-June during 2000–2004 (Tang et al., 2006). Zhu et al. (2005) reported that red tide (Chl > 20 mg m^{-3}) occurred over a large area offshore of the mouth of the Changjiang River in late June 2003. Our results for interannual variability of YOC SCHL corresponded to the dramatic increase in HABs offshore of the mouth in late spring 2000. No relationship was found between the maximum monthly SCHL and Changjiang River discharge from February to June in this area, suggesting that the spring bloom is more important than the influence of the

Changjiang River discharge in spring.

Monthly maximum YOC SCHL in spring in the middle of the Yellow Sea showed a significant increasing trend during the study period (Fig. 6A). Our previous study (Yamaguchi et al., 2012) found an increasing trend in summer standard SCHL in the middle of the Yellow Sea for the period 1998 to 2006. Lin et al. (2005) reported that dissolved inorganic nitrogen increased annually from 1976 to 2000 owing to precipitation and Changjiang River discharge. Furthermore, Son et al. (2011) reported that in recent times, spring Chl has been high in the middle of the Yellow Sea because of dumping since 1988; dumping supplies nutrients to ocean waters. Our present results indicate possible eutrophication of the Yellow Sea as a result of human activity.

On the other hand, Lin et al. (2005) reported that average Chl and primary production in the Yellow Sea during the period of 1996–1998 were lower than in the period of 1983–1986, although the data was limited. They suggested that the agent responsible for this drop in production may be climate change becuae it corresponds with increases in ocean temperature. Our observation period was more recent than the observation of Lin et al. (2005). The relative impacts of eutrophication and climate change should certainly be disentangled in future studies.

5. Concluding Remarks

There is a general need to study seasonal and spatial patterns of phytoplankton abundance in high suspended sediment condition. However, it

is difficult to use ocean color remote sensing for observing Chl in high suspended sediment areas because there is no good atmospheric correction and in-water algorithms. As YECS be the example, locally tuned SCHL algorithm with less influence by high nLw due to suspended sediment was used to study the interaction between Chl and TSM as well as the interanual variation of those.

TSM was dominated by fine particle due to resuspension in the Chinese and Korean coasts and around the Changjiang Bank from late fall to early spring. There were typical spring blooms in the middle of the Yellow Sea and to the east and south of the Changjiang Bank; these blooms also occurred offshore from the Changjiang River mouth and around the Changjiang Bank after resuspended sediment concentrations decreased. When the CDW extended from offshore of the Changjiang River mouth to east of the Changjiang Bank from July to August, TSM was dominated by phytoplankton and related organic particles in the CDW.

Offshore from the mouth, monthly averaged YOC SCHL from March to May showed a significant increasing trend corresponding to the increasing trend of red tides. In the middle of the Yellow Sea, the monthly maximum of YOC SCHL in spring increased significantly over the 10 years we studied, possibly reflecting eutrophication.

The YOC SCHL data were consistent with field observations. Therefore, YOC SCHL measures are reasonable datasets to study the phytoplankton dynamics in areas of moderate-high suspended sediment. However, further verification of this algorithm is

required by comparison with *in situ* data. There is also a need to develop improved in-water and atmospheric correction algorithms. This study is a good example to show that ocean color satellite data with proper algorithm is a power tool to understand phytoplankton dynamics in moderate-high suspended sediment area.

Acknowledgements

We thank NASA/DAAC for providing the SeaWiFS data. Joji Ishizaka was partly supported by Special Coordination Funds for Promoting Science and Technology from the Ministry of Education, Culture, Sports, Science and Technology, Japan..

References

Chen, C., Zhu, J., Beardsley, R.C., Franks, P.J.S., 2003. Physical–biological sources for dense algal blooms near the Changjiang River. Geophysical Research Letters, 30(10), 1515–1518.

Cloern, J. E., 1996. Phytoplankton bloom dynamics in coastal ecosystems: A review with some general lessons from sustained investigation of San Francisco Bay, California. Reviews of Geophysics., 34, 127–168.

Cloern, J.E., 1987. Turbidity as a control on phytoplankton biomass and productivity in estuaries. Continental Shelf Research, 7(11), 1367–1381.

Fichez, R., Jickells, T. D. & Edmunds, H. M., 1992. Algal blooms in the high turbidity, a

result of the conflicting consequences of turbulence on nutrient cycling in a shallow water estuary. Estuarine, Coastal and Shelf Science 35, 577–592.

Gong, G.-C., Wen, Y-H., Wang, B-W., Liu, G-J., 2003. Seasonal variation of chlorophyll *a* concentration, primary production and environmental conditions in the subtropical East China Sea, Deep Sea Research II, 50, 1219–1236.

Hu, C., Carder, K. L., & Muller-Karger, F. E. (2000). Atmospheric correction of SeaWiFS imagery over turbid coastal waters. Remote Sensing of Environment, 74, 195−206.

Jamet, C., H. Loisel, C. P. Kuchinke, K. Ruddick, G. Zibordi, and H. Feng. 2011. Comparison of three SeaWiFS atmospheric correction algorithms for turbid waters using AERONET-OC measurements, Remote Sensing Environment, 115(8), 1955–1965, doi:10.1016/j.rse.2011.03.018.

Jiao, N.Z., Yang, Y.H., Hong, N., Ma, Y., Harada, S., Koshikawa, H., Watanabe, M., 2005. Dynamics of autotrophic picoplankton and heterotrophic bacteria in the East China Sea. Continental. Shelf Research, 25(10), 1265–1279.

Kawahara, M., Uye, S.-I., Ohtsu, K., Iizumi, H., 2006. Unusual population explosion of the giant jellyfish *Nemopilema nomurai* (Scyphozoa: Rhizostomeae) in East Asian waters. Marine Ecological Progress Series, 307, 161–173.

Kim, H., Yamaguchi, H., Zhu, J., Okamura., K., Kiyomoto, Y., Tanaka, K., Kim, S-W., Park, T., Oh, I-S., Yoo, S., Ishizaka, J., 2009. The Changjiang Diluted Water (CDW) detected by satellite chlorophyll-*a*. Journal of Oceanography, 65, 129–135.

Kishino, M., Tanaka, A., Ishizaka, J., 2005. Retrieval of chlorophyll *a*, suspended solids

and colored dissolved organic matter in Tokyo Bay using ASTER data. Remote Sensing of Environment, 99, 66–74.

Kiyomoto, Y., Iseki, K., Okamura, K., 2001. Ocean color satellite imagery and shipboard measurements of chlorophyll *a* and suspended particulate matter distribution in the East China Sea. Journal of Oceanography, 57, 37–45.

Lin, C., Ning, J., Su, J., Lin, Y., Xu, B. 2005. Environmental changes and the responses of the ecosystems of the Yellow Sea during 1976-2000. Journal of Marine Systems, 55, 223–234.

O'Reilly, J.E., Maritorena, S., O'Brien, M.C., Siegel, D.A., Toole, D., Menzies, D., Smith, R.C., Mueller, J.L., Mitchell, B.G., Kahru, M., Chavez, F.P., Strutton, P., Cota, G.F., Hooker, S.B., McClain, C.R., Carder, K.L., Muller-Karger, F., Harding, L., Magnuson, A., Phinney, D., Moore, G.F., Aiken, J., Arrigo, K.R., Letelier, R., Culver, M. 2000. Ocean color chlorophyll a algorithms for SeaWiFS, OC2, and OC4: version 4. In: Hooker, S.B., Firestone, E.R. (eds) NASA Tech Memo 2000–206892, vol. 11. NASA Goddard Space Flight Center, Greenbelt, pp 9–23

Prieur, L. and Sathyendranath, S. 1981. An optical classification of coastal and oceanic waters based on the specific spectral absorption curves of phytoplankton pigments, dissolved organic matter, and other particulate materials. Limnology and Oceanography, 26, 671–689.

Siswanto, E., Tang, J., Yamaguchi, H., Ahn, Y.-H., Ishizaka, J., Yoo, S., Kim, S.-W., Kiyomoto, Y., Yamada, K., Chiang, C., Kawamura, H., 2011 Empirical ocean color

algorithms to retrieve chlorophyll-*a*, total suspended matter, and colored dissolved organic matter absorption coefficient in the Yellow and East China Seas. Journal of Oceanography, 67, 627–650, DOI 10.1007/s10872-011-0062-z.

Son, S., Wang, M., Shon, J., 2011. Satellite observations of optical and biologicalproperties in the Korean dump site of the Yellow Sea. Remote Sensing of Environment, 115, 562–572, doi:10.1016/j.rse.2010.10.002.

Sverdrup H.U., 1953. On conditions for the vernal blooming of phytoplankton. Journal du Conseil, Conseil Permanent International pour I' Exploration de la Mer, 18, 287–295.

Tang, D. L., Di, B.P., Wei, G., Ni, I.H., Oh, I.S., Wang, S.F., 2006. Spatial, seasonal and species variations of harmful algal blooms in the South Yellow Sea and East China Sea. Hydrobiologia, 568, 245–253.

Tassan S (1994) Local algorithms using SeaWiFS data for the retrieval of phytoplankton, pigments, suspended sediment, and yellow substance in coastal waters. Applied Optics, 33:2369–2378. doi: 10.1364/AO.33.002369

Wang, B.D., 2006. Cultural eutrophication in the Changjiang (Yangtze River) plume: history and perspective. Estuarine Coastal and Shelf Science, 69, 471–477.

Xie, S.-P., Hafner, J., Tanimoto, Y., Liu, W.T., Tokinaga, H., Xu, H., 2002. Bathymetric effect on the winter sea surface temperature and climate of the Yellow and East China Seas. Geophysical Research Letters 29, http://dx.doi.org/10.1029/.

Yamaguchi, H., H.-C. Kim, Y. B. Son, S. W. Kim, K. Okamura, Y. Kiyomoto, J. Ishizaka,

2012. Seasonal and summer-interannual variations of SeaWiFS chlorophyll *a* in the Yellow Sea and East China Sea. Progress in Oceanography. http://dx.doi.org/http://dx.doi.org/10.1016/j.pocean.2012.04.004.

Yang, Z.S., Lei, K., Guo, Z.G., Wang, H.J., 2007. Effect of a winter storm on sediment transport and resuspension in the distal mud area, the East China Sea. Journal of Coastal Research, 23, 310–318. doi:10.2112/03-0130.1.

Zhou, M.J., Shen, Z.L., Yu, R.C., 2008. Responses of a coastal phytoplankton community to increased nutrient input from the Changjiang (Yangtze) River. Continental Shelf Research, 28, 1483–1489.

Zhu, J.R., Wang, J.H., Shen, H.T. & Wu, H., 2005. Observation and analysis of the diluted water and red tide in the sea off the Changjiang River mouth in middle and late June 2003. Chinese Science Bulletin, 50, 240–247.

Zhu, Y., Chang, R., 2000. Preliminary study of the dynamic origin of the distribution pattern of bottom sediments on the continental shelves of the Bohai Sea, Yellow Sea and East China Sea. Estuarine, Coastal and Shelf Science, 51, 663–680.

Zhu, Z.-Y., Ng, W.-M., Liu, S.-M., Zhang, J., Chen, J.-C, Wu, Y. 2009. Estuarine phytoplankton dynamics and shift of limiting factors: a study in the Changjiang (Yangtze River) Estuary and adjacent area. Estuarine Coastal Shelf Science, 84, 393–401.

Figure captions

Figure 1. Map of the study area with bathymetry.

Figure 2. Distribution of 10-year average of monthly standard SCHL (mg m^{-3}) (A) and YOC SCHL (mg m^{-3}) (B), difference between YOC and standard SCHL (mg m^{-3}) (C), TSM (g m^{-3}) (D) and YOC SCHL/TSM (E) with bathymetry.

Figure 3. Seasonal variation in 10-year-averaged monthly YOC SCHL (mg m^{-3}) and TSM (g m^{-3}) along (A) 124.5°E and (B) 31.75°N lines. Gray color indicates no data.

Figure 4. Seasonal variation in 10-year averaged monthly YOC SCHL (mg m^{-3}) and TSM (g m^{-3}) from January to December in the middle of the Yellow Sea (A), south of the Changjiang Bank (B), offshore of the Changjiang River mouth (C), around the Changjiang Bank (D), and east of the Changjiang Bank (E). Black and white symbols indicate YOC SCHL and TSM, respectively.

Figure 5. Scatter diagrams between 10-year-averaged monthly YOC SCHL (mg m^{-3}) and TSM (g m^{-3}) in the middle of the Yellow Sea (A), south of the Changjiang Bank (B), offshore of the Changjiang River mouth (C), around the Changjiang Bank (D), and east of Changjiang Bank (E). Red dashed curves follow SCHL/TSM=1/500 for phytoplankton-dominated TSM in Tokyo Bay (Kishino et

al., 2005).

Figure 6. Interannual variation in monthly YOC SCHL (mg m^{-3}) and TSM (g m^{-3}) from February to June during 1998–2007 in the middle of the Yellow Sea (A), south of the Changjiang Bank (B), offshore of the Changjiang River mouth (C), around the Changjiang Bank (D), and east of the Changjiang Bank (E). Red and blue lines indicate YOC SCHL and TSM, respectively.

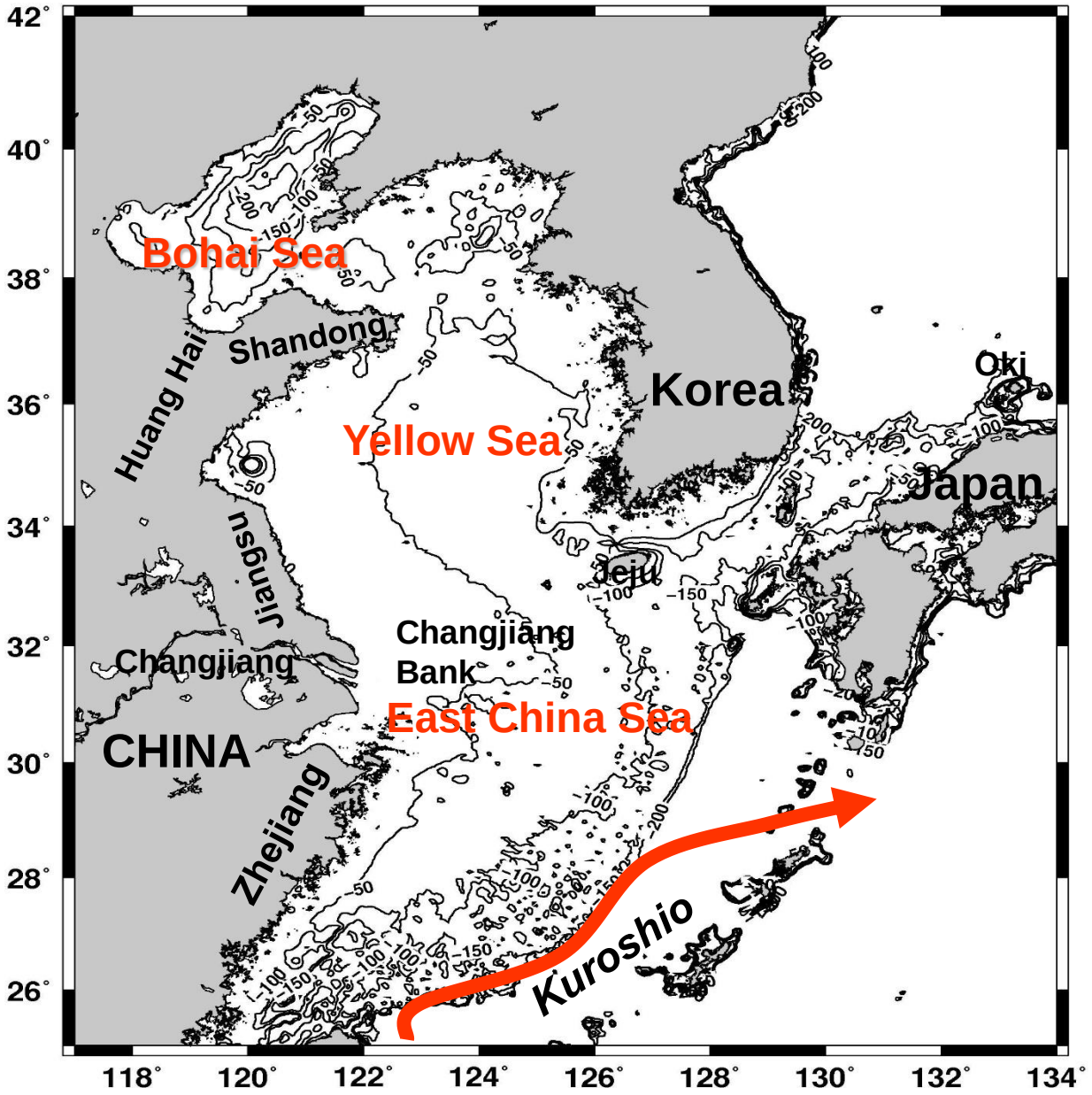
Bohai Sea
Huang Hai
Shandong
Yellow Sea
Korea
Oki
Japan
Jeju
Jiangsu
Changjiang
Changjiang Bank
East China Sea
CHINA
Zhejiang
Kuroshio
42°
40°
38°
36°
34°
32°
30°
28°
26°
118°
120°
122°
124°
126°
128°
130°
132°
134°

Fig. 1

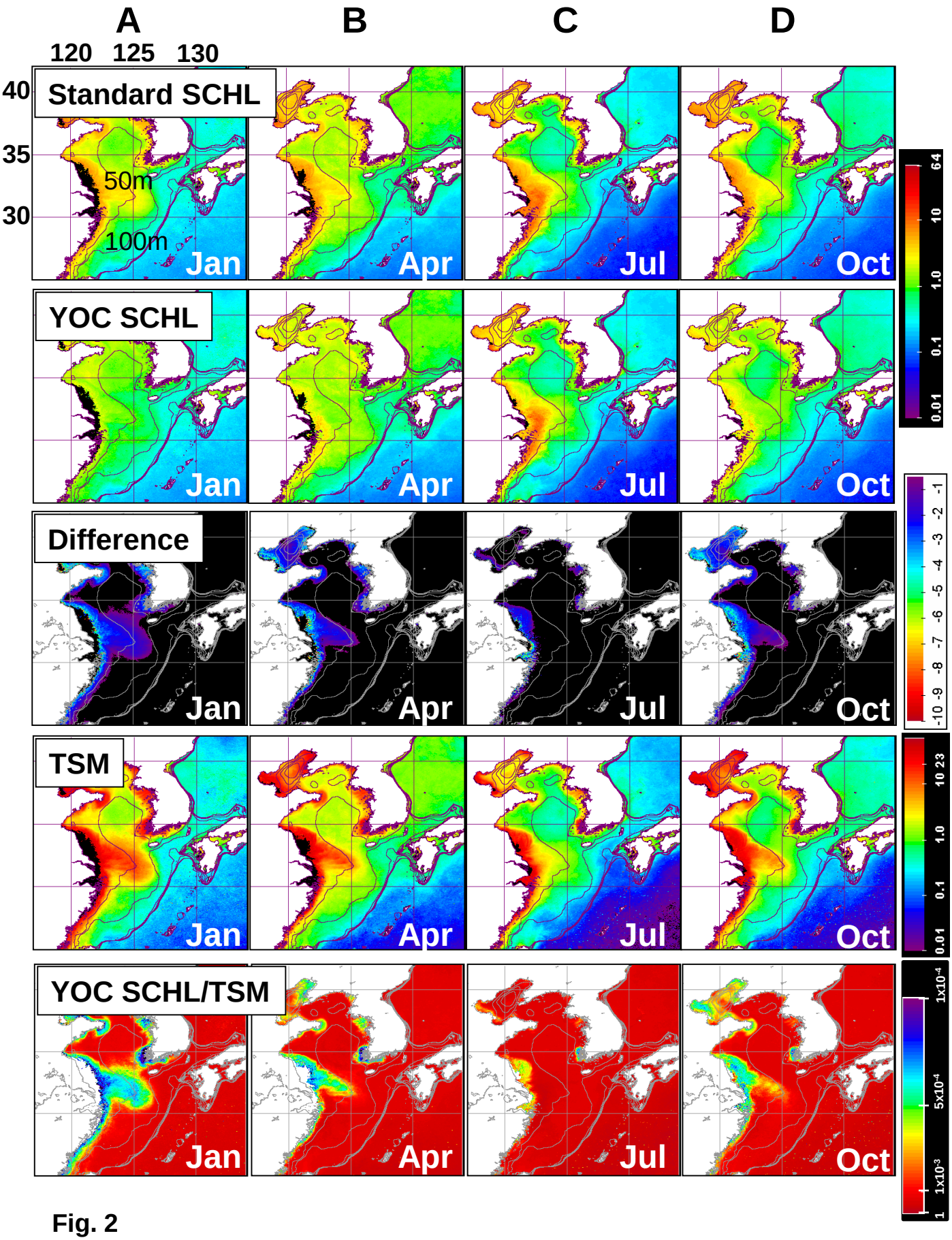
A
B
C
D
120
125
130
40
35
30
Standard SCHL
50m
100m
Jan
Apr
Jul
Oct
YOC SCHL
Difference
TSM
YOC SCHL/TSM
64
10
1.0
0.1
0.01
-1
-2
-3
-4
-5
-6
-7
-8
-9
-10
23
1x10-4
5x10-4
1x10-3
1

Fig. 2

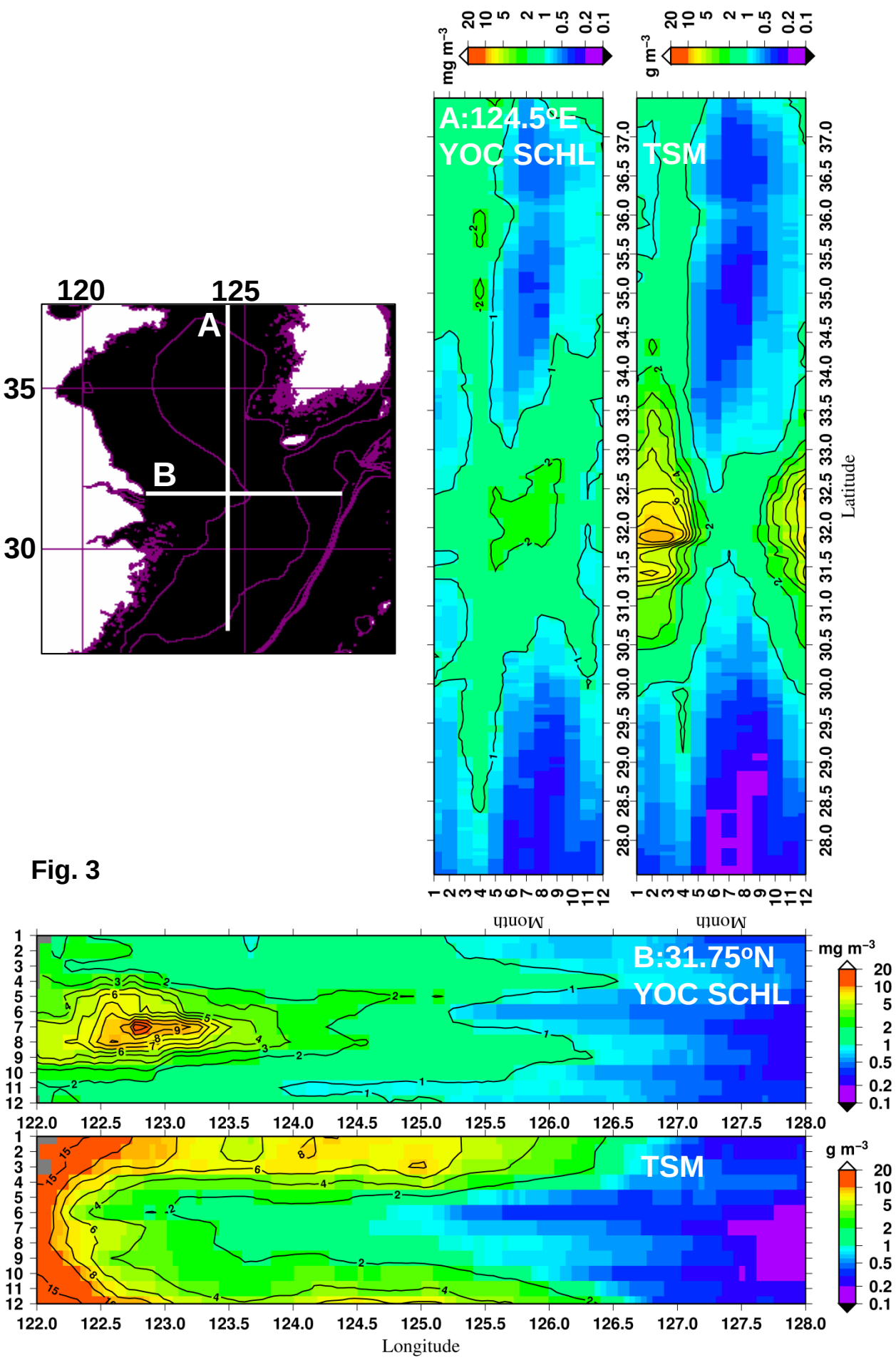
120
125
A
B
35
30
A:124.5°E
YOC SCHL
TSM
mg m⁻³
g m⁻³
20
10
5
2
1
0.5
0.2
0.1
Month
Latitude
B:31.75°N
YOC SCHL
TSM
Longitude
122.0
122.5
123.0
123.5
124.0
124.5
125.0
125.5
126.0
126.5
127.0
127.5
128.0

Fig. 3

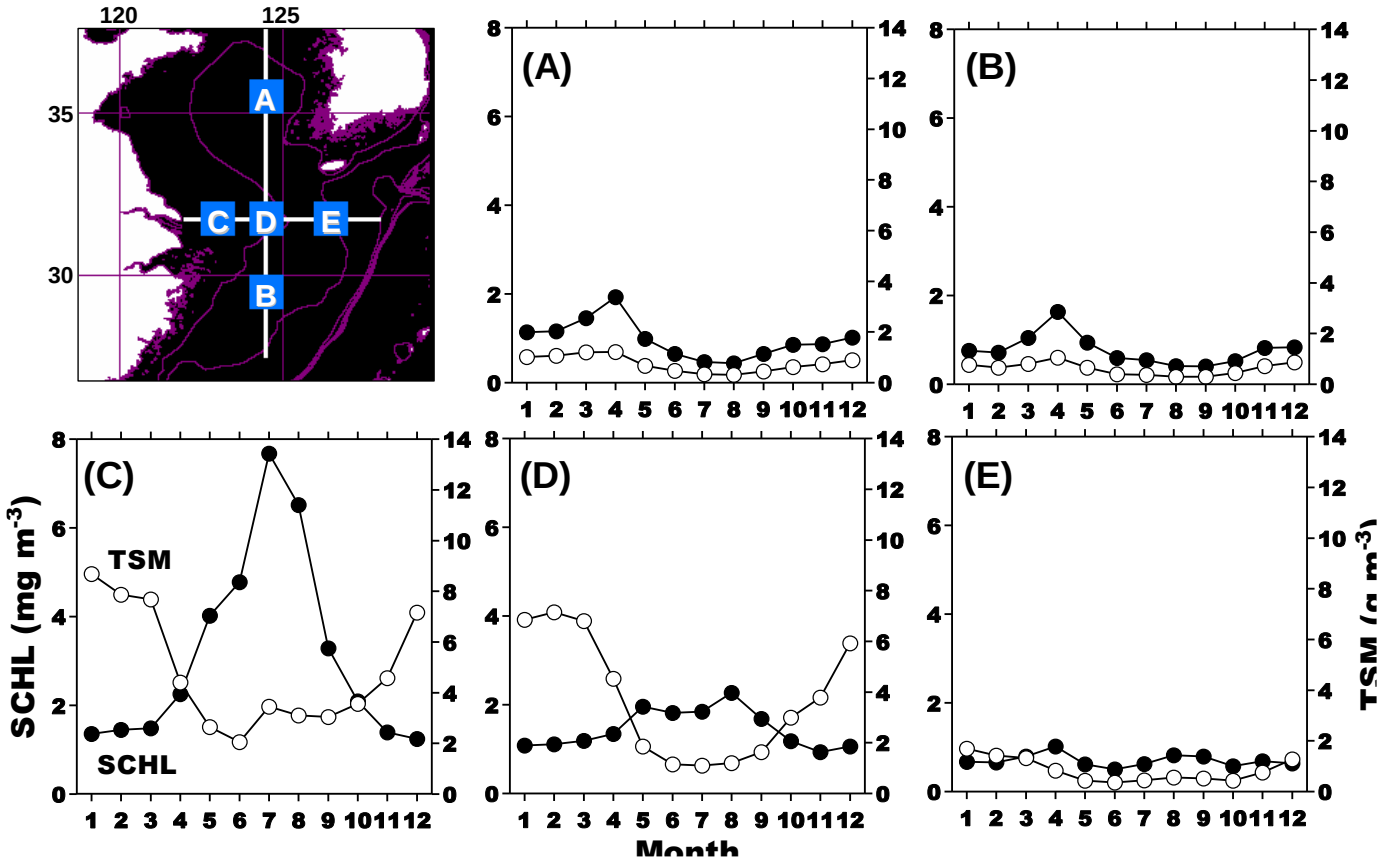

Fig. 4

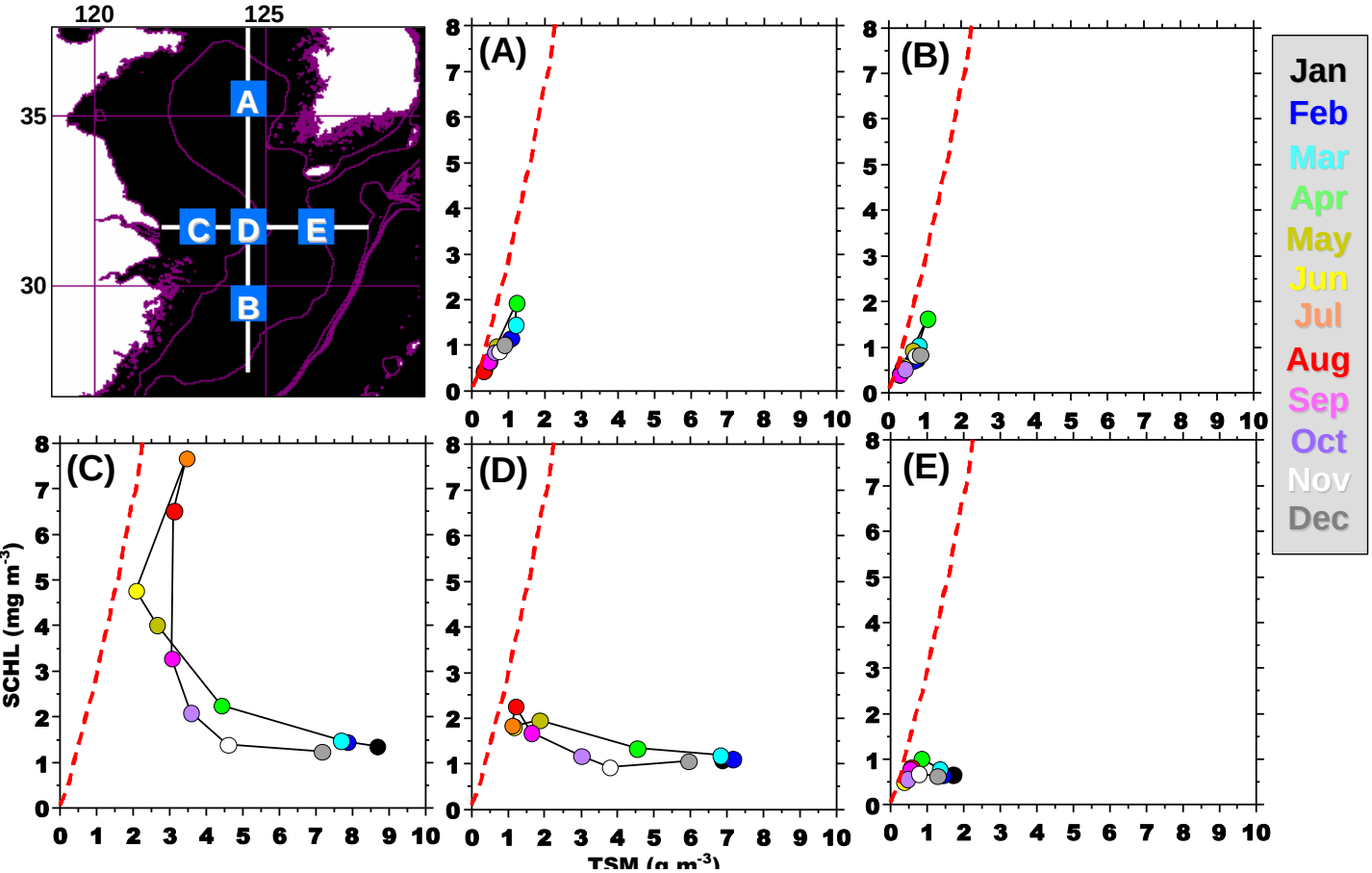
120
125
35
30
A
B
C
D
E
(A)
(B)
(C)
(D)
(E)
Jan
Feb
Mar
Apr
May
Jun
Jul
Aug
Sep
Oct
Nov
Dec
SCHL (mg m-3)
TSM (g m-3)

Fig. 5

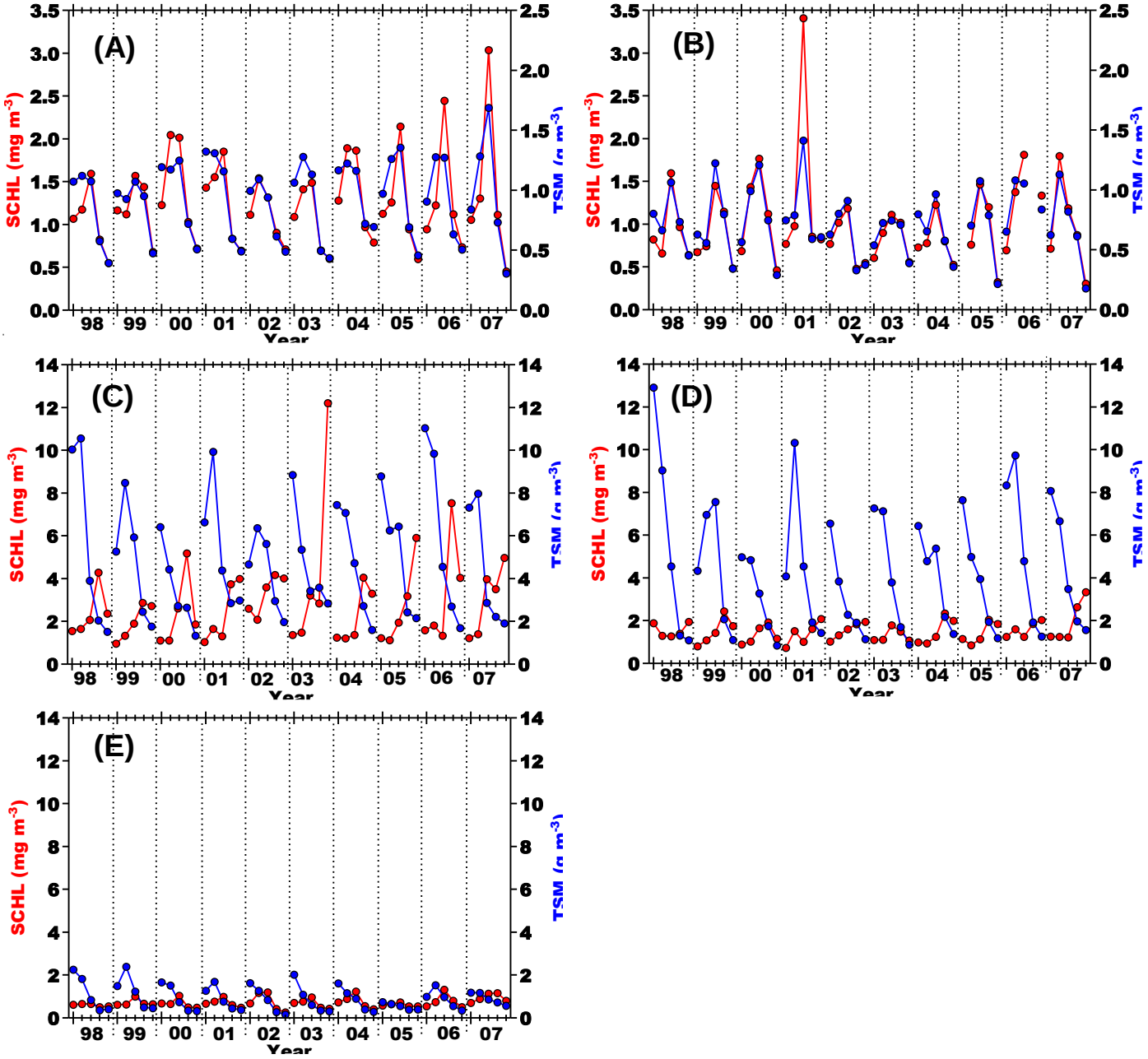

Fig. 6